A FINITE ELEMENT MODEL OF PERFORATED PANEL ABSORBERS INCLUDING VISCOTHERMAL EFFECTS

Jesús Carbajo[1], Jaime Ramis[1], Luís Godinho[2], Paulo Amado-Mendes[2], Jesús Alba[3]

[1]University of Alicante, Department of Physics, System Engineering and Signal Theory, 03080 Alicante, Spain, e-mail: {jesus.carbajo, jramis}@ua.es

[2]CICC, Department of Civil Engineering, University of Coimbra, 3030-788 Coimbra, Portugal, e-mail: {lgodinho, pamendes}@dec.uc.pt

[3]Higher Polytechnic School of Gandía, Department of Applied Physics, 46730 Grao de Gandía (Valencia), Spain, e-mail: {jesalba}@fis.upv.es

Keywords: Perforated panels; sound absorption; Navier-Stokes equations; FEM.

A FINITE ELEMENT MODEL OF PERFORATED PANEL ABSORBERS INCLUDING VISCOTHERMAL EFFECTS

ABSTRACT

Most of the analytical models devoted to determine the acoustic properties of a rigid perforated panel consider the acoustic impedance of a single hole and then use the porosity to determine the impedance for the whole panel. However, in the case of not homogeneous hole distribution or more complex configurations this approach is no longer valid. This work explores some of these limitations and proposes a finite element methodology that implements the linearized Navier Stokes equations in the frequency domain to analyze the acoustic performance under normal incidence of perforated panel absorbers. Some preliminary results for a homogenous perforated panel show that the sound absorption coefficient derived from the Maa analytical model does not match those from the simulations. These differences are mainly attributed to the finite geometry effect and to the spatial distribution of the perforations for the numerical case. In order to confirm these statements, the acoustic field in the vicinities of the perforations is analyzed for a more complex configuration of perforated panel. Additionally, experimental studies are carried out in an impedance tube for the same configuration and then compared to previous methods. The proposed methodology is shown to be in better agreement with the laboratorial measurements than the analytical approach.

1.   Introduction

Perforated panels backed by an air cavity and a rigid wall are sound absorbers commonly used in noise control applications. The sound absorption is produced by viscous losses in their pores so that, when reduced in size, they provide high acoustic resistance and low mass reactance necessary for a wide-band sound absorber. These systems have become an environmentally friendly alternative to fibers and foams, providing higher durability and enhancing sound absorption at low frequencies.

Numerous works have been dedicated to modeling the acoustic impedance of such devices [1-3], based on the model of sound propagation in narrow tubes studied by Crandall [4] and Rayleigh [5]. Most of these models determine the acoustic performance of this type of resonators from their orifice diameter, perforation rate, panel thickness and depth of the air gap. Although typically studied configurations consist of a flat rigid surface with periodically arranged circular holes or slits, some authors have proposed ways to model different perforation shapes or non-traditional designs of the perforated panel [6, 7]. Atalla and Sgard [8] have shown that a perforated plate or screen can be modeled as an equivalent fluid following the Johnson-Champoux-Allard approach [9, 10, 11] with an equivalent tortuosity and that those classical models can be reobtained by using this simple approach. Even though most of these models have been experimentally validated through the years, some uncertainties related to more complex configurations arise.

Some of the above analytical approaches are based on the assumption of no interaction effect between the perforations (widely separated holes). According to Rschevkin [12], Fok's function can be used to correct the reactive effect for the case of

interacting perforations. Nevertheless, in some cases this effect is linked to the porosity effect and is difficult to estimate its contribution isolated. For example, Miasa et al. [13] investigated experimentally the use of multiple sizes of holes in perforated panels. They observed that the sound absorption characteristics were enhanced and attributed this fact to the interaction effect, but did not compare the results with any theoretical model. In a recent work by Tayong [14], the effects of hole interaction along with heterogeneity distribution are investigated. In doing so, an inverse method is used to obtain the geometrical tortuosity that accounts for both effects and which is integrated in the characteristic impedance expression following Atalla and Sgard model. Cobo et al. [15] proposed a slight modification of the Maa and equivalent fluid models to deal with perforated panel manufactured by infiltration. Unfortunately, the main drawback of these latter studies is the requirement of some type of fitting procedure for the characterization of samples. To overcome these and other limitations in the characterization process, complementary modeling techniques must be developed.

Modeling the propagation of acoustic waves through narrow geometries such as orifices of perforated panels cannot neglect dissipative effects of viscous shear and heat conduction of the medium (air). Linearized Navier Stokes formulation, unlike isentropic/lossless acoustics governed by the Helmholtz equation, takes these viscothermal effects into account. The modeling of the behaviour of air in these situations requires the use of prediction methods that can handle this formulation. In this context, and given the progressive increase in the calculation speed of computers, the use of simulation techniques such as the Boundary Element Method (BEM) or the Finite Element Method (FEM) to approach these types of problems becomes feasible and can

4

be very useful.

Craggs and Hildebrandt [16] presented a simplified finite element model to solve Navier-Stokes equations for one-directional sound propagation in tubes of various shapes. Afterwards, Christensen et al. [17] compared different analytical and numerical models using as references two test cases with circular geometry, obtaining similar results for all models. Later on, Kierkegaard et al. [18] developed a methodology with a linearized Navier-Stokes equations solver in the frequency domain to efficiently simulate two-dimensional acoustic wave propagation in duct systems. The simulated results were compared to experimental data using a frequency scaling and showed an excellent agreement. More recently, Herdtle et al. [19] performed CFD (Computational Fluid Dynamics) estimations of the acoustic impedance of microperforated panels for different hole designs using an axisymmetric model generated parametrically, but did not compare the results with any experimental work.

The main disadvantage of the finite element discretization of the full viscothermal acoustic formulation is its high computational cost, since a large number of elements is needed to properly model thermal and viscous boundary layers. Notwithstanding this problem, and although other more efficient models as the Low Reduced Frequency (LRF) model have been used to describe viscothermal propagation in simple tube or layer geometries [20], the full model offers a wide applicability since no geometric restrictions are imposed for the calculations. So as to increase the computational efficiency compared to the full model, Kampinga et al. [21] presented an approximate model that can also be used for arbitrary geometries. Moreover, as the analytical models of perforated panel absorbers represent the extreme situation in which the resonant

system is infinitesimal, through the use of a finite element procedure the effect of the finite geometry on the absorption performance can be captured. Therefore, the finite element modeling of perforated panels with viscothermal acoustics represents an interesting alternative for those complex configurations in which no estimation models are available.

The main aim of this work is to estimate the absorption performance of different perforated panel systems using a frequency domain finite element methodology for viscothermal acoustics. The study is focused on thin rigid panels with circular shaped holes and does not consider mean flow or any motion of the plate. In order to validate the proposed characterization methodology, the sound absorption coefficient under normal incidence is determined for the analysed configurations. The results are then compared to a well-established analytical model and to experimental measurements performed by means of an impedance tube. The experiments are performed in the range of sound pressure level where the linear impedance model is valid, showing a good agreement when compared to the model simulations.

The structure of the paper is as follows; in section 2, the Maa impedance model for the case of perforated panels backed by an air cavity is reviewed; in section 3, the set of linearized Navier-Stokes equations in the frequency domain for viscothermal acoustics and their finite element implementation are briefly introduced, and in section 4 the numerical setup implemented for the simulations is described; then, in section 5, the proposed methodology is compared with the analytical model for a test case and validated through measurements in an impedance tube for different perforated panel configurations; finally, section 6 describes the main conclusions of this paper.

6

2.   Acoustic impedance of a perforated panel absorber

Fig. 1 shows a schematic representation of a rigid perforated panel excited by a plane wave and immersed in a fluid medium. The panel is assumed to be of infinite extent and composed by a periodic distribution of identical cylindrical perforations of circular cross-section.

FIGURE 1

The classical approaches to analyse such systems consist in evaluating the acoustic impedance of a single perforation and then use the porosity to determine the impedance for the whole panel. This complex impedance will depend mainly on the perforation rate ϕ, perforation diameter d and panel thickness t. Its resistive part is induced by the viscous boundary layers within the perforations and at the panel surface, and by the flow distortion effects generated at the edges of each hole, while the reactive part accounts for the inertia effects from the motion of air cylinders in the holes of the panel. The previously described phenomena are included in both real and imaginary parts of impedance as additive terms or multiplicative factors, depending on the analytical model. One common particularity of most of these models is that they consider small thickness and shape of the perforations so that thermal energy loss can be considered to be negligible compared to viscous loss. Moreover, they are based on the underlying assumption that no interaction exists between neighbouring holes. Such assumption may not be appropriate if the holes are fairly close, and so a modification of the impedance expression using Fok's function may be used. These aspects are satisfied in the linear

regime, where the sound levels are low and the particle velocity is not so high.

Maa proposed a well-known equation for the acoustic impedance Z of perforated panels whose dimensions are small compared to the wavelength of a normal incident sound wave

$$Z = \frac{\sqrt{2}\eta k}{\phi d} + j\frac{\omega \rho_0}{\phi}\left[\frac{0.85d}{\psi(\xi)} + t\left(1 - \frac{2J_1\left(k\sqrt{-j}\right)}{k\sqrt{-j}J_0\left(k\sqrt{-j}\right)}\right)^{-1}\right], \tag{1}$$

where ρ_0 is the air density, ω the angular frequency, η the dynamic viscosity of air, $k = d\sqrt{\rho_0\omega/4\eta}$ the perforate constant, J_0 and J_1 are Bessel functions of the first kind and zeroth and first orders respectively, $j = \sqrt{-1}$ the imaginary unit, and $\psi(\xi)$ the Fok function, given by

$$\psi(\xi) = \left(1 - 1.40925\xi + 0.33818\xi^3 + 0.06793\xi^5 - 0.02287\xi^6 + 0.03015\xi^7 - 0.01641\xi^8 + ...\right)^{-1}, \tag{2}$$

with $\xi = 0.88d/b$, being b the distance between perforations.

Perforated panels require a rigid wall spaced a distance D to create a resonant system with a relatively broadband absorption. The normal surface impedance Z_S of the perforated panel-air cavity combination can be written as

$$Z_S = Z - j\rho_0 c_0 \cot\left(\frac{\omega D}{c_0}\right), \tag{3}$$

where c_0 is the sound propagation velocity in air.

The sound absorption coefficient α of the perforated panel absorber for the case of normal incidence, defined by the ratio of the absorbed to the incident sound energies, can be expressed in terms of the normal surface impedance as follows

$$\alpha = 1 - \left|\frac{Z_S - \rho_0 c_0}{Z_S + \rho_0 c_0}\right|^2. \tag{4}$$

3.   Viscothermal acoustics

3.1   The linearized Navier Stokes equations

The propagation of sound in narrow tubes, such as those that form a perforated panel, lead to significant boundary layer viscous and thermal effects that slow down acoustic waves and cause a strong damping for frequencies near the resonance of the absorber system. Even though viscous effects cause more damping than the thermal effects, both actively contribute to the acoustic damping. Nevertheless, for most viscothermal acoustic problems, thermal energy loss is negligible compared to viscous loss [20, 22]. These effects are typically neglected in the isotropic wave equation, which assumes adiabatic and inviscid behaviours. The Navier Stokes equations describe mathematically this viscothermal wave propagation and can be simplified to a time harmonic form that enables forward transformation to the frequency domain for a harmonic analysis.

9

The set of equations to be linearized consists of conservation of momentum, conservation of energy and conservation of mass together with the constitutive equations of state for an ideal gas. Although the linearized formulation is to be given without mathematical derivations, since it is beyond the scope of this work (see [22] for further details), some of the assumptions that must be highlighted are: density, temperature and pressure variations are considered small compared to their constant average values, the convective derivative is also small compared to all other variations and viscous dissipation does not contribute to the energy balance. On the other hand, no mean flow, small perturbations and a homogeneous medium are assumed. Wave propagation is therefore considered from a standard acoustical point of view and non-linear effects are neglected.

The resulting linearized governing equations for the case of an ideal gas not subjected to body forces and transformed to the frequency domain can be written as

$$j\omega\rho_0\mathbf{v} = -\nabla p + (\lambda + \mu)\nabla(\nabla\cdot\mathbf{v}) + \mu\Delta\mathbf{v}, \tag{5}$$

$$j\omega\rho_0 C_p T = j\omega p + \kappa\Delta T, \tag{6}$$

$$j\omega\left(\frac{p}{p_0} - \frac{T}{T_0}\right) + \nabla\cdot\mathbf{v} = 0. \tag{7}$$

where $\mathbf{v}$ is the velocity vector, p the pressure, T the temperature; ρ_0, p_0 and T_0 are constant average values for density, pressure and temperature respectively; λ is the second coefficient of viscosity, μ is the coefficient of shear viscosity, C_p denotes the specific heat at constant pressure and κ the coefficient of thermal conductivity. It

should be noted that an additional identity known as the Gibbs relation is used to present these equations in a form with pressure, temperature and velocity as degrees of freedom.

Moreover, appropriate viscothermal boundary conditions must be prescribed on each boundary location. In viscothermal acoustics these boundary conditions typically correspond to adiabatic (no heat flow) pressure sources, $-\mathbf{n}\cdot\left(-\kappa\nabla T\right)=0$, being $\mathbf{n}$ the unit vector normal to that boundary, and rigid isothermal walls (null velocity and temperature) where the no-slip condition is applied over the fluid-rigid interface, $\mathbf{v}=\mathbf{0}$, and temperature variations vanish, $T=0$.

3.2   Finite element implementation

The Finite Element Method (FEM) is a widely used method to numerically solve partial differential equations. The present finite element implementation corresponds to an existing method [23] with a differently scaled energy equation that results in an unsymmetrical system matrix, but is reported here for completeness. A finite element model that implements a boundary value problem for Eqs. (5) - (7) requires writing those equations in a weak form. This can be accomplished by using a Galerkin approach: multiplication of these equations by the weighting functions $\mathbf{v}_w$, T_w and p_w respectively, and integration over the problem domain before application of Green's theorem to reduce the order of the derivatives. Boundary conditions (velocity and temperature) must be prescribed explicitly. The resulting weak form reads

$$j\omega\rho_0\left\langle \mathbf{v}_w,\mathbf{v}\right\rangle+2\mu\left\langle \varepsilon_w,\varepsilon\right\rangle+\lambda\left\langle \nabla\cdot\mathbf{v}_w,\nabla\cdot\mathbf{v}\right\rangle-\left\langle \nabla\cdot\mathbf{v}_w,p\right\rangle=$$
$$\left\langle \mathbf{v}_w,\left(\lambda\left(\nabla\cdot\mathbf{v}\right)\mathbf{I}+2\mu\varepsilon-p\mathbf{I}\right)\cdot\mathbf{n}\right\rangle_{\partial\Omega},\tag{8}$$

$$-j\omega\rho_0 C_p\left\langle T_w,T\right\rangle-\kappa\left\langle \nabla T_w,\nabla T\right\rangle+j\omega\left\langle T_w,p\right\rangle=\left\langle T_w,-\kappa\left(\nabla T\right)\cdot\mathbf{n}\right\rangle_{\partial\Omega},\tag{9}$$

$$-\frac{j\omega}{p_0}\left\langle p_w,p\right\rangle-\left\langle p_w,\nabla\cdot\mathbf{v}\right\rangle+\frac{j\omega}{T_0}\left\langle p_w,T\right\rangle=0,\tag{10}$$

where $\varepsilon=0.5\left(\nabla\mathbf{v}+\left(\nabla\mathbf{v}\right)^{\mathrm{T}}\right)$ is the symmetric part of the velocity gradient , ε_w is defined like ε

by replacing $\mathbf{v}$ by $\mathbf{v}_w$ and $\mathbf{I}$ is the identity tensor. Eqs. (8) – (10) use the inner products over

the domain Ω and its boundary $\partial\Omega$, which are given by

$$\left\langle \mathbf{z}_w,\mathbf{z}\right\rangle_{\Omega}\equiv\int_{\Omega}\overline{\mathbf{z}_w}\cdot\mathbf{z}d\Omega,\tag{11}$$

$$\left\langle \mathbf{z}_w,\mathbf{z}\right\rangle_{\partial\Omega}\equiv\int_{\partial\Omega}\overline{\mathbf{z}_w}\cdot\mathbf{z}d\partial\Omega,\tag{12}$$

being $\mathbf{z}$ a dummy vector. The overbar denotes the complex conjugate. For scalars and

tensors, the dot product is replaced by the scalar and the double dot product,

respectively. The weak form results in the system matrix

$$\begin{bmatrix} \mathbf{M}_{1,1} & 0 & \mathbf{M}_{1,3} \\ 0 & \mathbf{M}_{2,2} & \mathbf{M}_{2,3} \\ \mathbf{M}_{3,1} & \mathbf{M}_{3,2} & \mathbf{M}_{3,3} \end{bmatrix}\begin{Bmatrix} \vec{\mathbf{v}} \\ \vec{T} \\ \vec{p} \end{Bmatrix}=\begin{Bmatrix} \vec{\mathbf{f}} \\ \vec{Q} \\ 0 \end{Bmatrix},\tag{13}$$

where $\vec{\mathbf{v}}$, $\vec{T}$ and $\vec{p}$ are the vectors of the nodal values; the sub-matrices entries $\mathbf{M}_{i,j}$ and

the right hand side of Eq. (13), which contains the natural boundary conditions, are derived from Eqs. (8 – 10).

The resulting weak form is then discretized by using a linear combination of shape functions (typically Lagrangian) to approximate the solution, the boundary conditions and the weighting functions. The governing viscothermal acoustic equations together with the relevant boundary conditions are implemented in the finite element commercial software COMSOL Multiphysics® and solved using the PARDISO direct solver.

The use of a finite element model based on the full linearized Navier Stokes equations exhibits a series of advantages over approximate (often analytical) models as it can be used to any class of geometries and their accuracy is only limited by the discretization errors inherent to FEM. The use of the above so-called mixed formulation (it contains both velocity and pressure degrees of freedom) provides a more stable and robust behaviour of the method. Its main drawback is the very large amount of computing resources required for optimal convergence rate. The finite element model performance also depends on the element shape and the order of polynomial functions used, as well as on the mesh refinement and the boundary conditions that must be met. Some details regarding these aspects are given in the next section.

4.   Numerical setup

The acoustic behaviour of perforated panel absorbers under normal incidence is investigated by using a finite element procedure that implements the linearized Navier Stokes equations in the frequency domain. The modeling procedure described below is based on a simple and easy to analyse configuration that consists of two cylindrical

volumes separated by the test specimen and which represent an impedance tube and a backing cavity, as shown schematically in Fig 2a.

FIGURE 2

The acoustic field inside the duct is coupled with that in the backing cavity via the air motion inside the orifices and is governed by the aforementioned equations. The duct length is $L = 1000$ mm and both the duct and the cavity have a radius $a = 50$ mm. The cavity depth D and perforated panel parameters depend on the configuration under study. For all cases, symmetry can be used and only one eight of the geometry has to be modeled (Fig. 2b). The boundary condition to be enforced on the symmetry boundary planes is $\mathbf{n} \cdot \mathbf{v} = 0$. The perforated panel and the walls of the duct and the cavity are assumed to be rigid (no-slip condition) and isothermal. In this numerical scheme, the excitation is introduced by an adiabatic pressure source placed at the left hand boundary of the numerical setup, as a radiating plane surface. The simulations have been performed for frequencies up to 500 Hz with a 10 Hz frequency step, since this range can adequately describe the absorption range of the absorber system. The pressure responses at two points, placed at 235 mm and 150 mm away from the specimen under test, are registered to obtain the transfer function and calculate the sound absorption coefficient and impedance under normal incidence following the ISO 10534-2 standard [24].

As the main purpose of this work is to check if the finite element methodology allows studying the acoustic performance of perforated panel absorbers for practical

design purposes, it is important to give some additional details concerning the finite element discretization. Since creating adequate boundary layer mesh in 3D geometries is not an easy task, tetrahedral Taylor-Hood-like elements have been used instead with a relatively higher element density near the outer and inner walls of the perforated panel, so as to capture its viscous and thermal boundary layer effects. The mesh used for the viscothermal finite element model is depicted in Fig. 3. The largest elements, located at the impedance tube and the cavity, were 6 cm long, and the wavelength of the highest computed frequency (f_{max} = 500 Hz) was $\lambda = c/f_{max}$ = 341.2/500 = 68 cm, which yields an element per wavelength ratio of 68/6 ≈ 11, for the worst case. The smallest elements are located at the perforations and are 0.022 cm long, which gives more than 3000 elements per wavelength for the highest frequency. The elements' length was not small enough to resolve the viscous and thermal boundary layer thicknesses, but acceptable for the studied cases as will be shown in Section 5.

FIGURE 3

The whole computational domain consists of a total of around 80000 elements, yielding more than 500000 degrees of freedom. In the current implementation, a stable solution was obtained by using linear Lagrange shape functions for the pressure while the other variables were approximated by quadratic Lagrange shape functions. Using equal order shape functions for all degrees of degrees of freedom would result in an unstable element discretization [22].

The highest time consumption for one frequency was around 284 s on a 16 core 2.26

GHz, 24 GByte RAM workstation. It should be noted that since the finite element code corresponds to a commercial package, it was not possible to accurately assess the memory used by the application for the calculation itself; and the solution time given was reported by the simulation software. Hence, though the frequency domain linearized Navier-Stokes formulation is immensely computationally demanding for very detailed simulations and needs to be performed with great care, fairly reliable results can be obtained using a relatively coarse mesh.

5.   Results and discussion

5.1   Test case

As a preliminary evaluation of the viscothermal finite element modeling procedure, the sound absorption characteristics of a perforated panel absorber are simulated. The test case consists of a flat rigid homogeneous perforated panel with periodically arranged circular holes whose properties are $\phi = 0.79$ %, $d = 4$ mm, $t = 1$ mm, $b = 40$ mm and with a constant air gap $D = 50$ mm. The choice of these geometrical parameters is arbitrary but valid to demonstrate the distinct acoustic properties of the perforated panel absorber.

A mesh study has been performed previously to determine the required mesh size such that the results become nearly mesh-independent. Despite using an unstructured mesh, the element size is decreased, especially close to the perforated panel inner boundaries, until the results converge to a stable value. Simulations were computed for different number of degrees of freedom and the absorption coefficient is obtained using the finite element procedure presented above.

16

FIGURE 4

The results depicted in Figure 4 show a relative convergence to the finest mesh with each mesh refinement. Thus, although a suitable choice of the mesh is required so as not to lead to unreliable results, the discretization herein used is shown to be acceptable.

The numerical model is then compared with the analytical solution of Maa described in Section 2. For such configuration, the normal incidence sound absorption coefficient and surface impedance can be calculated analytically from Eqs. (1) − (4). Likewise, these parameters are obtained numerically. To highlight the different results produced by the numerical model and by the more classical analytical approach, the two perforated panel spatial arrangements shown in Fig. 5 are evaluated.

FIGURE 5

The effect of this change of the spatial arrangement of the perforated panel in the cross section of the tube is linked to the porosity but this issue is not taken into account in the theoretical model since it assumes the perforated panel to be immersed in a semi-infinite fluid media. The predicted results of absorption coefficient and imaginary part of the normalized surface impedance for these configurations are compared in Fig. 6a and Fig. 6b, respectively.

FIGURE 6

17

The presented results reveal that the finite element simulation is not in agreement with the analytical solution. Theoretical sound absorption coefficient calculated by using the Maa model yields an absorption peak of 0.34 at 336 Hz, whereas the numerical model yields a greater maximum sound absorption coefficient shifted to a lower frequency of 320 Hz for the PPSA1 and to 290 Hz for the PPSA2. Notice that the decreasing porosity of the PPSA2 from the PPSA1 forces the central frequency of the absorption coefficient band lower in frequency and the peak value to increase. Moreover, the shift of the peak towards the low frequency range is a result of the increase of the system added mass as observed in the imaginary part of the normalized surface impedance in Fig. 6b.

Since small thickness of perforations makes thermal energy loss negligible, these differences can be mainly attributed to the finite geometry modeling effect of the proposed methodology when compared to the analytical model, which represents the extreme situation in which the perforated panel absorber is infinitesimal. In the next subsection, it will be shown that this factor poses a serious difficulty in obtaining a good estimation for more complex configurations and that the simulation results are more consistent than the analytical values when compared to experimental data from measurements in an impedance tube.

5.2   Experimental validation

In a following step and for verification purposes, experimental measurements of various methacrylate perforated panel absorbers are carried out in an impedance tube

following the ISO 10534-2 standard [24]. The calculated absorption coefficients are compared with those obtained from the viscothermal finite element model and the Maa analytical model.

The specimens under study show a heterogeneous spatial pattern of the holes (unevenly distributed perforations) and are rigid enough to satisfy the rigid assumptions of the Maa model. This particular design is mainly intended to stand out the potential of the proposed numerical methodology for the case of complex configurations with respect to analytical solutions. The dimensions of three of the measured samples whose results are shown in this work are listed in Table 1 and a picture of one of the specimens is shown in Fig. 7.

TABLE 1

FIGURE 7

The experimental setup for measuring the normal incidence absorption coefficient is the same as that described in Section 4 for the numerical models and consists of a circular cross section tube with a thickness of 6 mm. The cut-off frequency of the tube is around 1990 Hz. A loudspeaker is located at one end of the tube and the perforated panel system is attached at the other end. A random excitation is provided to the loudspeaker from the analyser (OR34 Compact Analyser) and the pressure transfer function is measured using two pressure microphones of 1/2 inch (B&K Type 4188) mounted flush with the inner surface of the tube at two locations. Since the acoustic

19

analysis of the present study is based upon linear models, the incident sound pressure level in the impedance tube has been kept below 90 dB. The frequency range of analysis was chosen to ensure plane wave propagation and avoid excitations of higher modes. The resultant sound absorption coefficient of the perforated panel absorber system is then obtained.

Fig. 8 compares the measured absorption coefficient to those calculated numerically and analytically.

FIGURE 8

The absorption curves on Fig. 8 show that the viscothermal finite element model can accurately describe the absorption performance for the analysed configurations. The results might be improved by using a finer mesh but both measurements and simulated results show a good agreement. On the other hand, the analytical model is not as accurate as expected and hardly matches the measured maximum absorption peak for these particular perforated panel absorbers. This is partly because the spatial pattern of the holes of the perforated panel is heterogeneous and the flange conditions are not equal for neighbouring holes.

To illustrate this statement and to better understand the acoustic behaviour near the perforated panel, the acoustic field has been examined numerically with the aid of the finite element model for the perforated panel absorber PP1. Fig. 9 shows a cross-sectional overview of the magnitude distribution and streamlines of the velocity field in the region of geometric discontinuities (the perforations) at the resonance frequency

20

$f = 350$ Hz.

FIGURE 9

The complex distributions of both axial and transverse velocities at the discontinuities illustrate dominant dissipation mechanisms. As can be seen from Fig. 9a, the axial component in between the discontinuities has a constant velocity far from the rigid walls, increasing as it gets closer to the walls and decaying to zero on the walls. A close-up of the transversal velocity is shown in Fig. 9b, which reveals how the acoustic field is distorted in the near field of the perforated panel because of the inertia effects but distinctly for each hole since the flange conditions differ from an on axis perforation to one located near the contours of the impedance tube or the backing cavity.

Hence, the prediction of the absorption characteristics of perforated panels using a general analytical approach might not be suitable when the spatial arrangement of the perforations makes the flange and interaction effects play a significant role. For these cases, a more detailed analysis should be carried out carefully. The use of a finite element methodology as proposed in this paper can be an interesting alternative to standard models, which is quite general and applicable to a wider range of geometry cases.

6.   Conclusions

A viscothermal finite element modeling procedure that implements the linearized Navier Stokes equations in the frequency domain has been proposed to evaluate the

21

sound absorption performance under normal incidence of perforated panel absorbers as an alternative to analytical approaches. The presented model is necessary to predict wave propagation in fluids through narrow arbitrary geometries where viscous and thermal effects cannot be neglected.

Initially, the absorption coefficient and acoustic impedance of a perforated panel absorber are simulated and compared with the analytical solution of the Maa model. In order to clarify the differences between the numerical model and the theory, several heterogeneous perforated panel samples have been manufactured and tested in an impedance tube. It was found that the experimental results are in better agreement with the numerical predictions that the analytical approach for these perforated panel designs. The resonance frequencies of the absorbers are also more precisely determined by the numerical model. The difference can be mainly attributed to the effect of the spatial arrangement of the perforations and their flange conditions in the absorption mechanism of the perforated panel absorber. Contour maps, at a frequency of interest, confirm this hypothesis and show that such models can be helpful for the analysis of the sound field in the vicinities of the perforated panel and to clearly understand the roles of finite size and interaction effect.

The main advantage of the methodology is that it is generic and it can handle perforated panel systems of arbitrary geometry in a straightforward manner, without the need of fitting procedures or modified formulations. The mesh could be refined to give even more accurate predictions but the feasibility of such models is reasonably validated. However, further research must be carried out in this area to minimize the required computational resources and to reduce the problem size as much as possible

through more efficient models. Anyway, results show that the developed models give a good estimation of the acoustic behaviour of these resonator systems and can thus be applied in practice to optimize their design when no analytical solution exists.
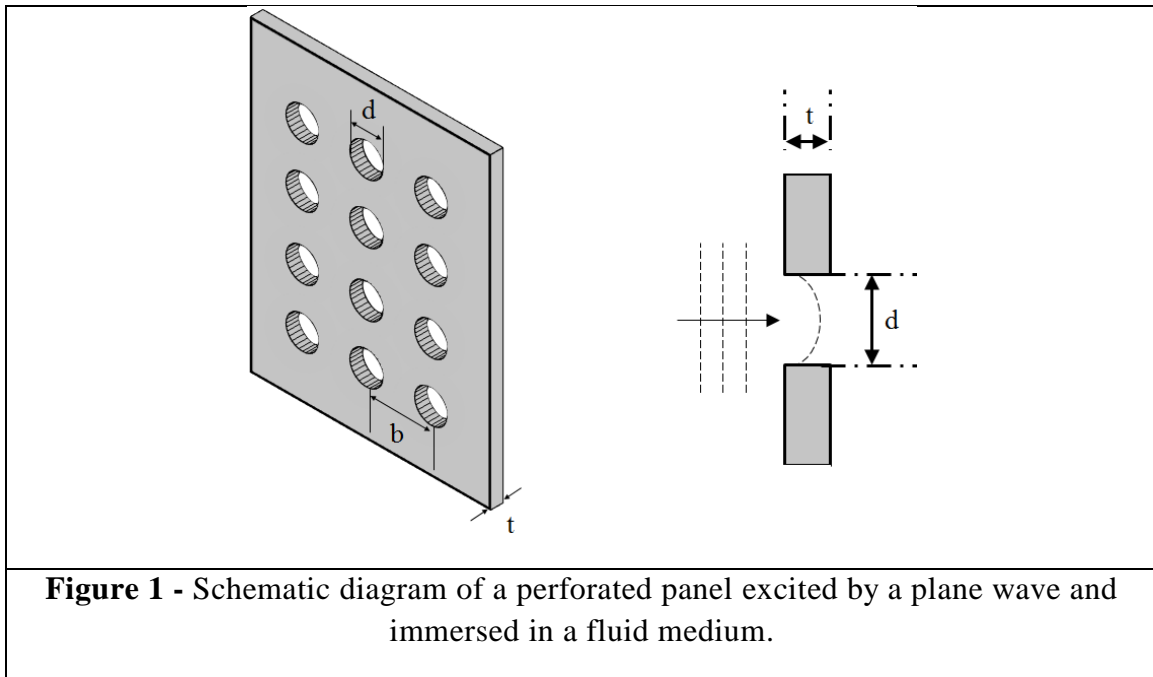
References

[1]   Maa DY. Microperforated wideband absorbers, Noise Control Engineering Journal 1987; 29 (3): 77-84.

[2]   Beranek LL. Noise and vibration control engineering. New York: John Wiley and Sons; 1992.

[3]   Ingard U. Notes on sound absorption technology. Noise control foundation. New York: Poughkeepsie; 1994.

[4]   Crandall IB. Theory of vibrating systems and sound. New York: Van Notrand; 1926.

[5]   Rayleigh L. Theory of sound. 2nd ed. New York: Dover Publications; 1945.

[6]   Randeberg RT. Perforated panel absorbers with viscous energy dissipation enhanced by orifice design. PhD Thesis, Trondheim, Norway; 2000.

[7]   Sakagami K, Nagayama Y, Morimoto M, Yairi M. Pilot study on wideband sound absorber obtained by combination of two different microperforated panel (MPP) absorbers. Acoustical Science and Technology 2009; 30 (2): 154-56.

[8]   Atalla N, Sgard F. Modeling of perforated plates and screens using rigid frame porous models. Journal of Sound and Vibration 2007; 303: 195-208.

[9]   Johnson DL, Koplik J, Dashen R. Theory of dynamic permeability and tortuosity in fluid-saturated porous media. Journal of Fluid Mechanics 1987; 176: 379-402.

[10] Champoux Y, Allard JF. Dynamic tortuosity and bulk modulus in air-saturated porous media. Journal of Applied Physics 1991; 70 (4): 1975-79.

[11] Allard JF, Atalla N. Propagation of sound in porous media. Modelling sound absorbing materials. Wiley, Chichester, United Kingdom; 2009.

[12] Rschevkin SN. A course of lectures on the theory of sound. London: Pergamon Press; 1963.

[13] Miasa IM, Okuma M, Kishimoto G, Nakahara T. An experimental study of a multi-size microperforated panel absorber. Journal of System Design and Dynamics 2007; 1 (2): 331-9.

[14] Tayong R. On the holes interaction and heterogeneity distribution effects on the acoustic properties of air-cavity backed perforated plates. Applied Acoustics 2013; 74: 1492-8.

[15] Cobo P, Montero de Espinosa F. Proposal of cheap microperforated panel absorbers manufactured by infiltration. Applied Acoustics 2013; 74: 1069-75.

[16] Craggs A, Hildebrandt JG. Effective densities and resistivities for acoustic propagation in narrow tubes. Journal of Sound and Vibration 1984; 92 (3): 321-31.

[17] Christensen R, Juhl P, Cutanda Henriquez V. Practical modeling of acoustic losses in air due to heat conduction and viscosity. Euronoise 2008, Paris, France; 2008.

[18] Kierkegaard A, Boij S, Efraimsson G. A frequency domain linearized Navier-Stokes equations approach to acoustic propagation in flow ducts with sharp edges. Journal of the Acoustical Society of America 2010; 127 (2): 710-9.

24

[19] Herdtle T, Bolton JS, Kim NN, Alexander JH, Gerdes RW. Transfer impedance of microperforated materials with tapered holes. Journal of the Acoustical Society of America 2013; 134 (6): 4752-62.

[20] Beltman WM. Viscothermal wave propagation including acousto-elastic interaction. Dissertation, University of Twente, Enschede; 1998.

[21] Kampinga WR, Wijnant YH, de Boer A. An efficient finite element model for viscothermal acoustics. Acta Acustica united with Acustica 2011; 97 (4): 618-31.

[22] Kampinga WR. Viscothermal acoustics using finite elements: analysis tools for engineers. PhD Thesis, University of Twente, Netherlands; 2010.

[23] Kampinga WR, Wijnant YH, de Boer, A. Performance of several viscothermal acoustic finite elements. Acta Acustica united with Acustica 2010; 96 (1); 115-124.

[24] ISO 10534-2. Determination of sound absorption coefficient and impedance in impedance tubes (International Organization for Standardization), Switzerland; 1998.

Table 1 – Parameters of the perforated panel absorbers used in the experimental validation.

	ϕ (%)	d (mm)	t (mm)	b (mm)	D (mm)
PP1	1.77	1.6	3	5	70
PP2	1.35	1.4	3	5	90
PP3	0.99	1.2	3	5	110

Figure 1 - Schematic diagram of a perforated panel excited by a plane wave and immersed in a fluid medium.

(a)

(b)

Figure 2 - Schematic representation of the numerical setup: (a) Impedance tube and backing cavity separated by the perforated panel, with a pressure source at the left side of the tube; (b) Detailed frontal view with the assumed symmetry boundaries.
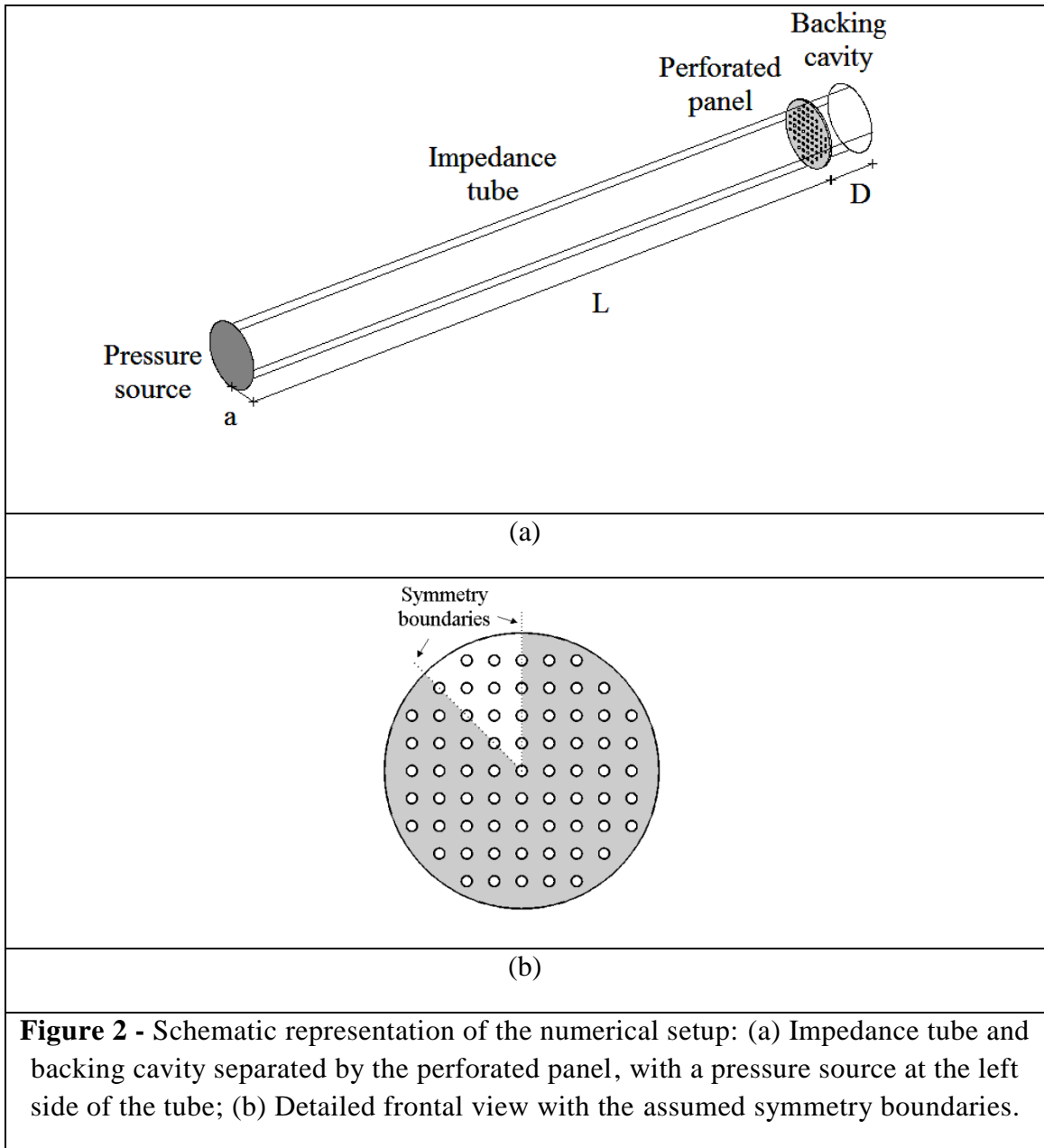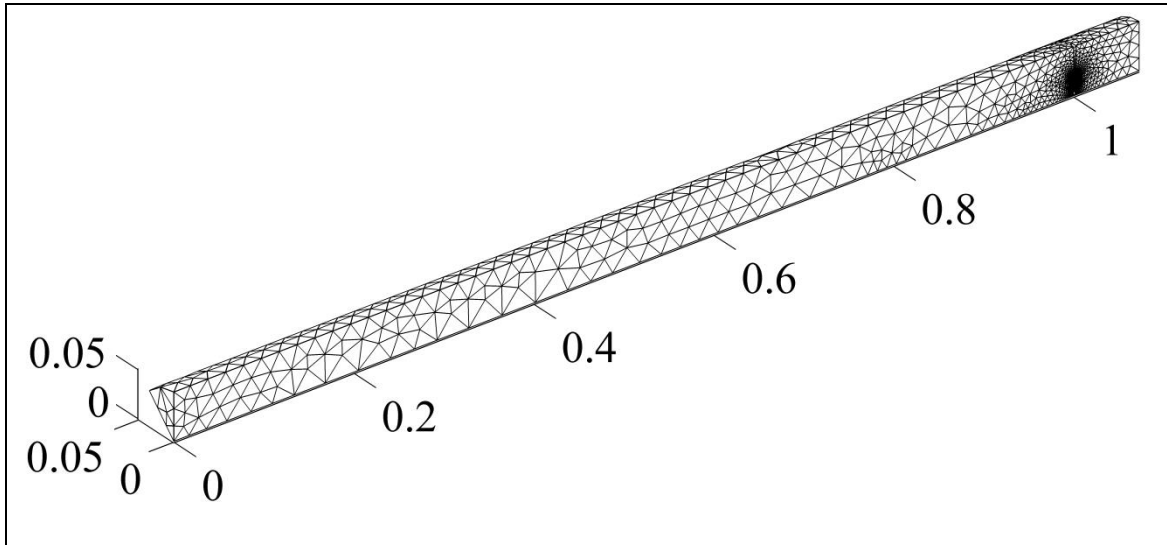
(a)
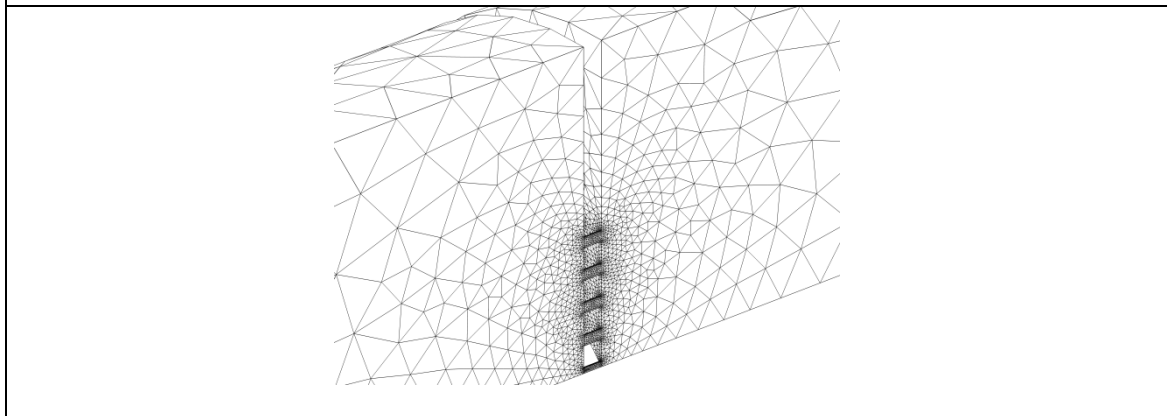
(b)

Figure 3 – Mesh used for the viscothermal finite element model: (a) General and (b) detailed view.
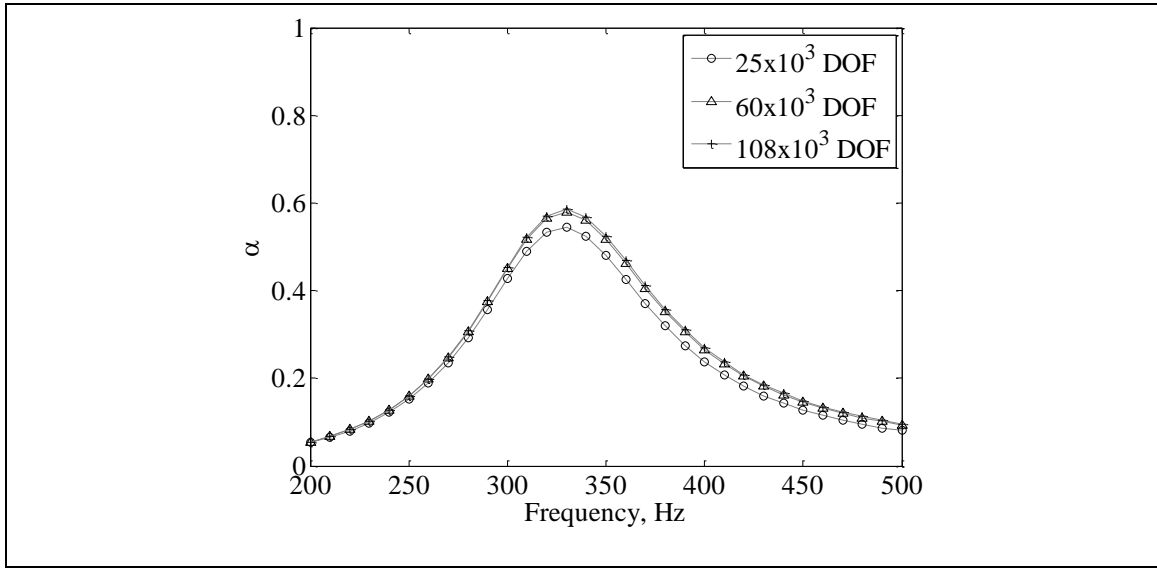
Figure 4 – Comparison of the simulation results for different mesh refinements of the normal incidence sound absorption coefficient for the test case of a perforated panel absorber.
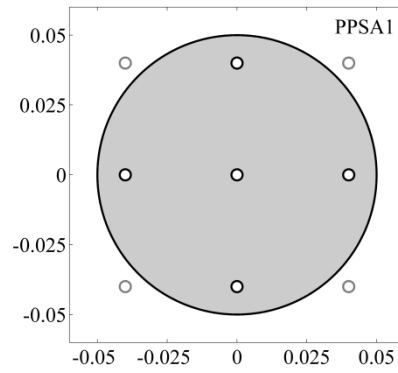
(a)
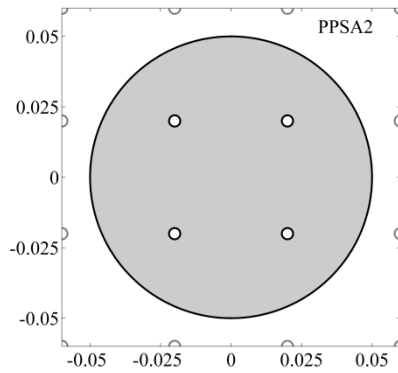
(b)

**Figure 5** – Detailed frontal view of the perforated panel spatial arrangements simulated: (a) PPSA1 and (b) PPSA2.
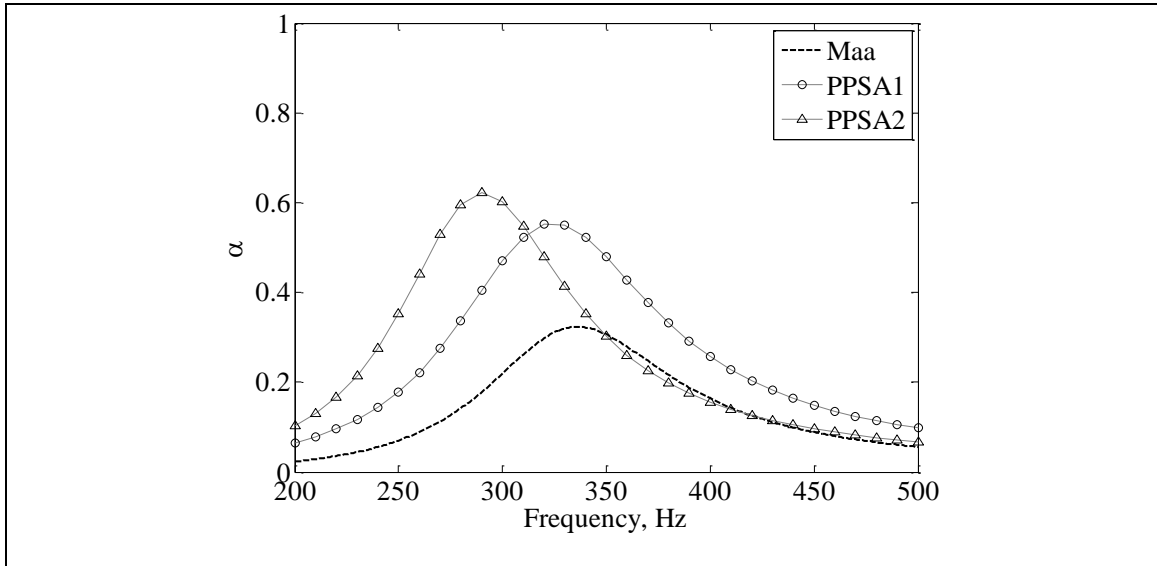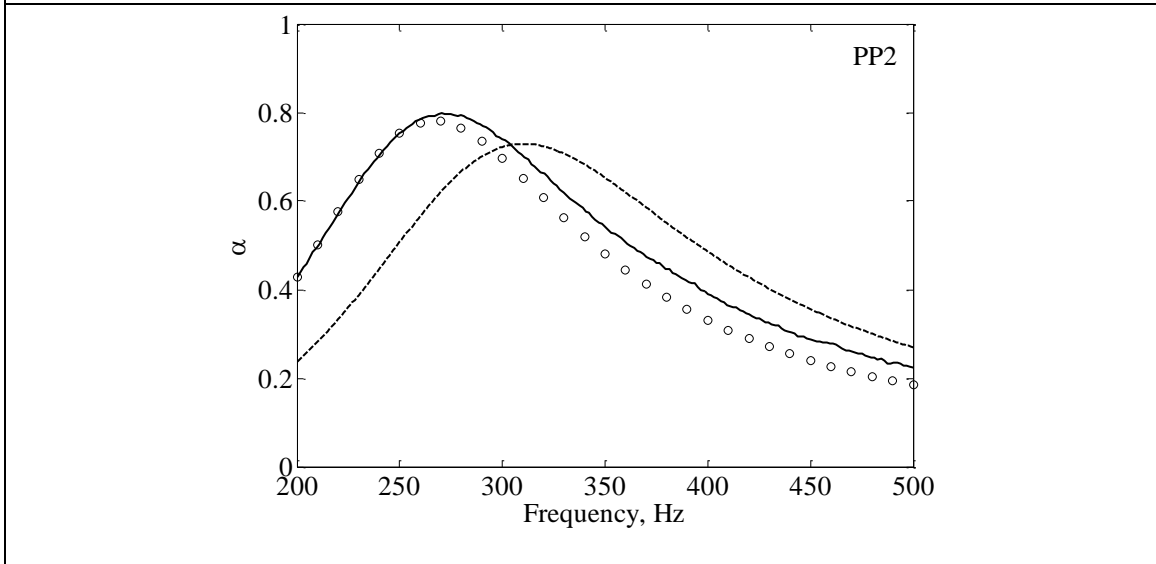
(a)
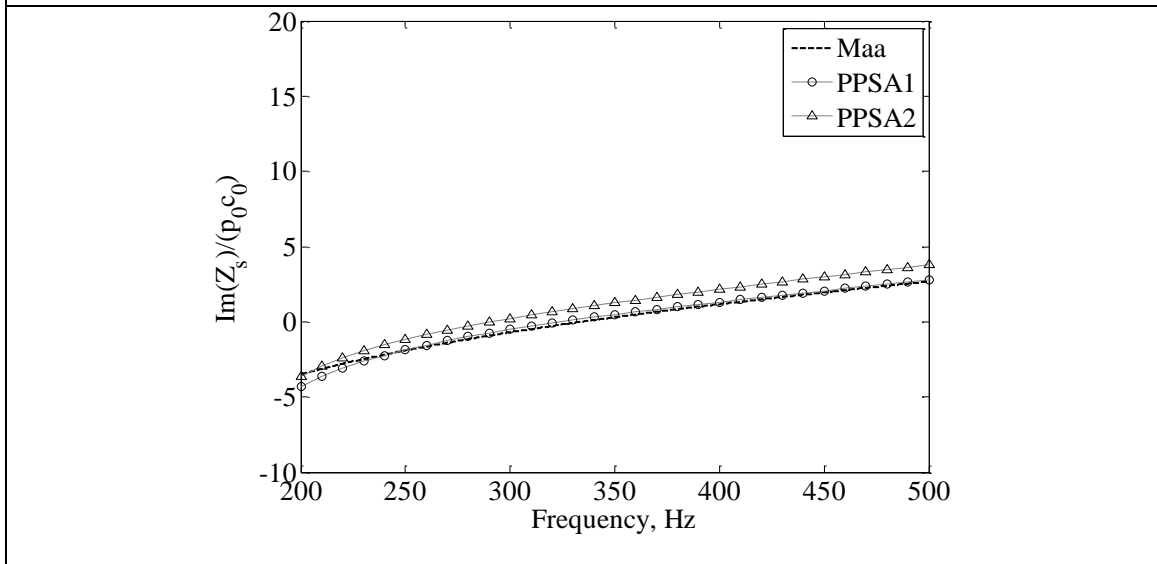
(b)

Figure 6 – Comparison of the analytical and simulated results for the test case of a perforated panel absorber: (a) normal incidence sound absorption coefficient and (b) imaginary part of the normalized surface impedance.
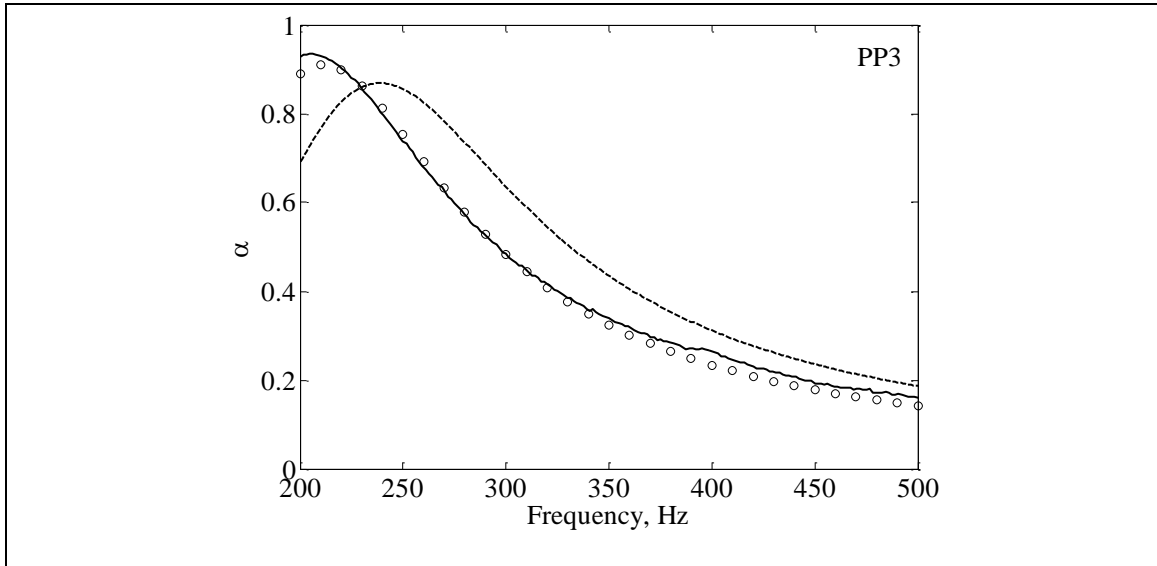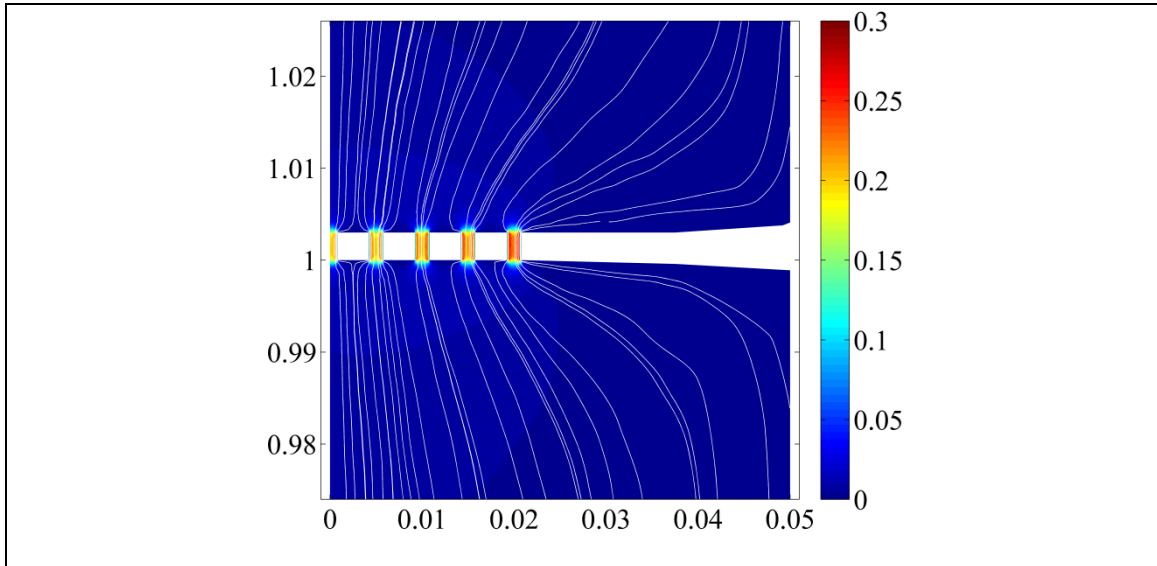
Figure 7 – Photograph and close-up picture of specimen used for perforated panel absorber PP2.
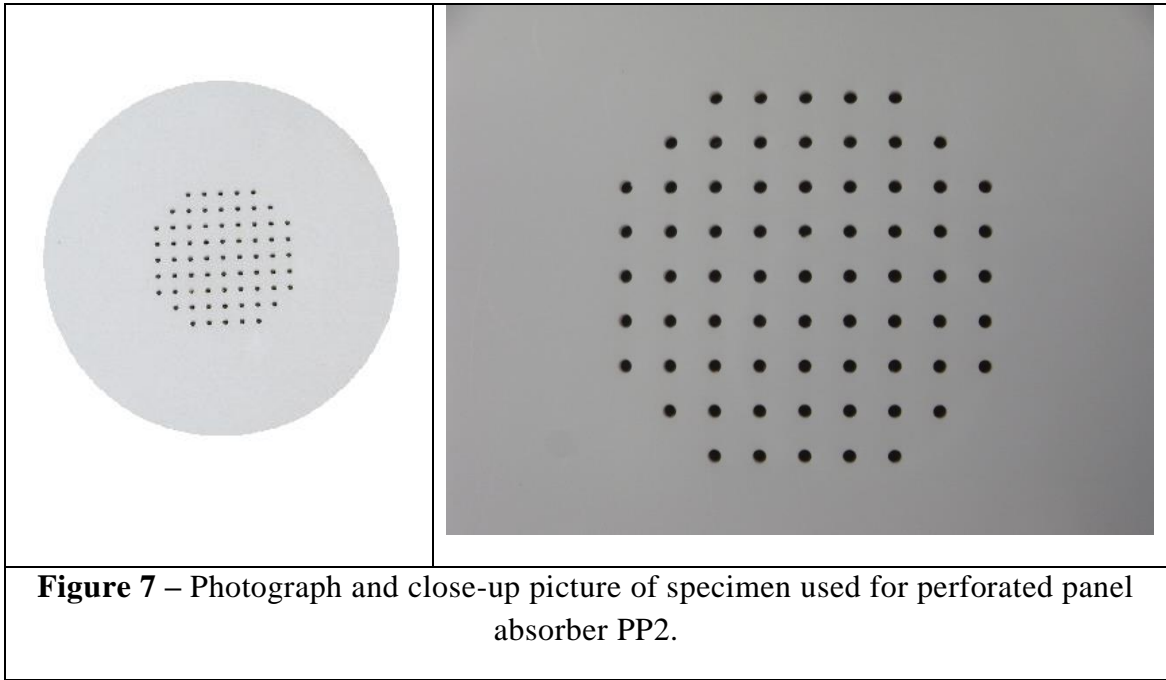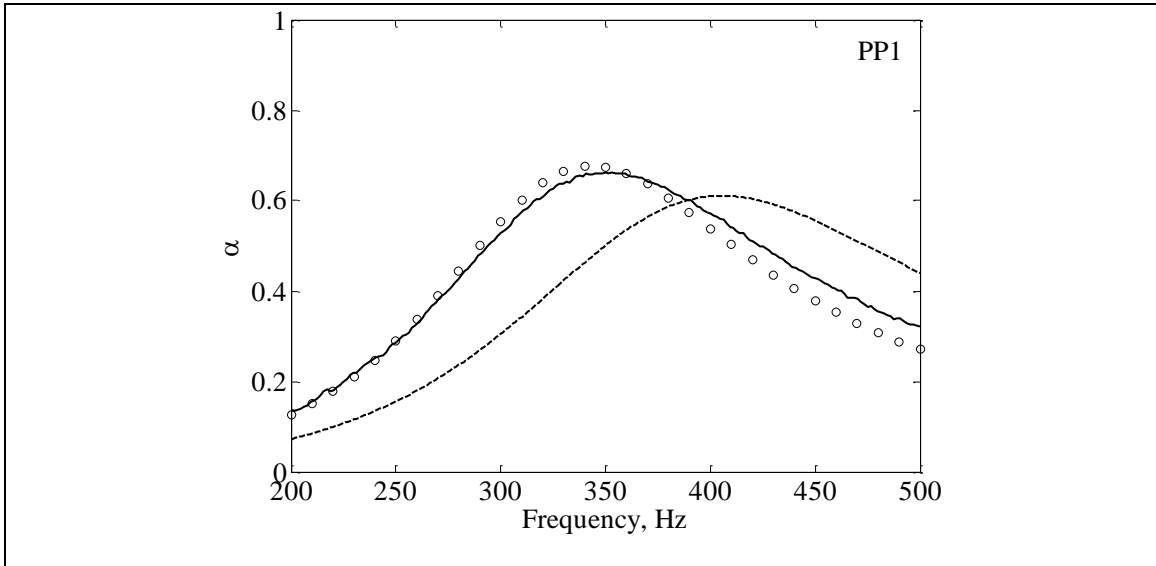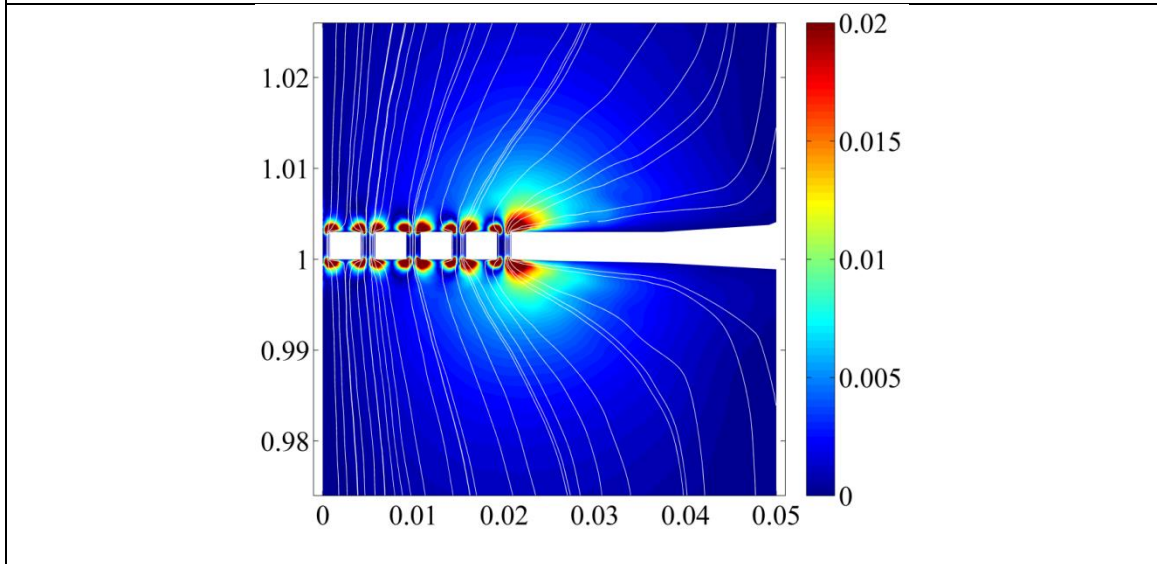
(a)

(b)

(c)

Figure 8 – Normal incidence sound absorption coefficient of three perforated panel absorbers: (a) PP1; (b) PP2 and (c) PP3 (see Table 1). Dashed line: Maa model; dots: numerical results; continuous line: measured values in experimental setup.

(a)

(b)

Figure 9 – Cross-sectional overview of the magnitude distribution of the velocity axial (a) and transverse (b) components with streamlines, at 350 Hz, for the perforated panel absorber PP1.